JACS
JOURNAL OF THE AMERICAN CHEMICAL SOCIETY
Article
pubs.acs.org/JACS

Compartmentalized Droplets for Continuous Flow Liquid–Liquid Interface Catalysis

Ming Zhang,[†,‡] Lijuan Wei,[†] Huan Chen,[†] Zhiping Du,[#] Bernard P. Binks,[§] and Hengquan Yang*[,†]

[†]School of Chemistry and Chemical Engineering, Shanxi University, Taiyuan 030006, China
[‡]Institute of Molecular Science, Shanxi University, Taiyuan 030006, China
[#]Institute of Resources and Environment Engineering, Shanxi University, Taiyuan 030006, China
[§]Department of Chemistry, University of Hull, Hull HU6 7RX, U.K.

Supporting Information

ABSTRACT: To address the limitations of batch organic–aqueous biphasic catalysis, we develop a conceptually novel method termed Flow Pickering Emulsion, or FPE, to process biphasic reactions in a continuous flow fashion. This method involves the compartmentalization of bulk water into micron-sized droplets based on a water-in-oil Pickering emulsion, which are packed into a column reactor. The compartmentalized water droplets can confine water-soluble catalysts, thus "immobilizing" the catalyst in the column reactor, while the interstices between the droplets allow the organic (oil) phase to flow. Key fundamental principles underpinning this method such as the oil phase flow behavior, the stability of compartmentalized droplets and the confinement capability of these droplets toward water-soluble catalysts are experimentally and theoretically investigated. As a proof of this concept, case studies including a sulfuric acid-catalyzed addition reaction, a heteropolyacid-catalyzed ring opening reaction and an enzyme-catalyzed chiral reaction demonstrate the generality and versatility of the FPE method. Impressively, in addition to the excellent durability, the developed FPE reactions exhibit up to 10-fold reaction efficiency enhancement in comparison to the existing batch reactions, indicating a unique flow interface catalysis effect. This study opens up a new avenue to allow conventional biphasic catalysis reactions to access more sustainable and efficient flow chemistry using an innovative liquid–liquid interface protocol.

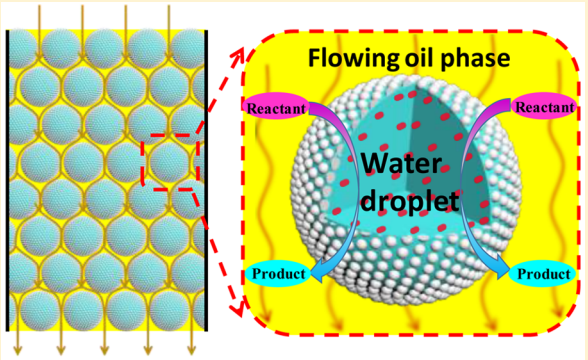

1. INTRODUCTION

Organic–aqueous biphasic catalysis reactions are extensively used in laboratory synthesis and in industrial fabrication of various chemicals because of their intrinsic advantages such as the simultaneous tolerance of water-soluble and oil-soluble reactants and the ease of recycling water-soluble catalysts.[1−7] However, due to the macroscopic phase separation driven by the high interfacial energy of the immiscible phases, biphasic reactions typically require external mechanical agitation to mix the two phases and maintain a large reaction interface during workup, which has to be implemented in batch reactors.[8] However, from a practical point of view, continuous flow processes are preferred, particularly in terms of productivity, mixing efficiency, safety and process control.[9−16] Nonetheless, due to the extreme challenge in preventing phase separation during flow, breakthroughs up to date in this context are only achieved in microfluidic and advanced flow technology[17−21] and the supported-aqueous-phase method.[22,23] In microfluidic and advanced flow systems, coflow or segmented flow of two phases is realized through micron-sized channel geometry restriction that prevents macroscopic phase separation. In the supported-aqueous-phase systems, a thin water film containing catalysts is adsorbed on a porous hydrophilic solid material or entrapped in an organogel, which is further packed into a fixed bed. Despite significant advances, these methods still rely on special/expensive equipment or materials. Hence, the development of a more straightforward and practical method to translate biphasic reactions from a batch fashion to a continuous flow manner is still a big challenge.

It is well-known that an organic–aqueous biphasic mixture can form a water-in-oil or oil-in-water Pickering emulsion in the presence of solid particles as emulsifier which are partly wettable by both oil and water.[24−29] In this system, one liquid is compartmentalized by a layer of particles to numerous micrometer-sized droplets (dispersed phase) that are dispersed uniformly in the other liquid (continuous phase), leading to a high organic–aqueous interfacial area. In comparison to conventional surfactant-stabilized droplets, those droplets compartmentalized by particles are highly stable to coalescence due to the high energy of detachment of particles from the interface.[30] More interestingly, the compartmentalized droplets,

Received: April 26, 2016
Published: July 18, 2016

DOI: 10.1021/jacs.6b04265
J. Am. Chem. Soc. 2016, 138, 10173−10183

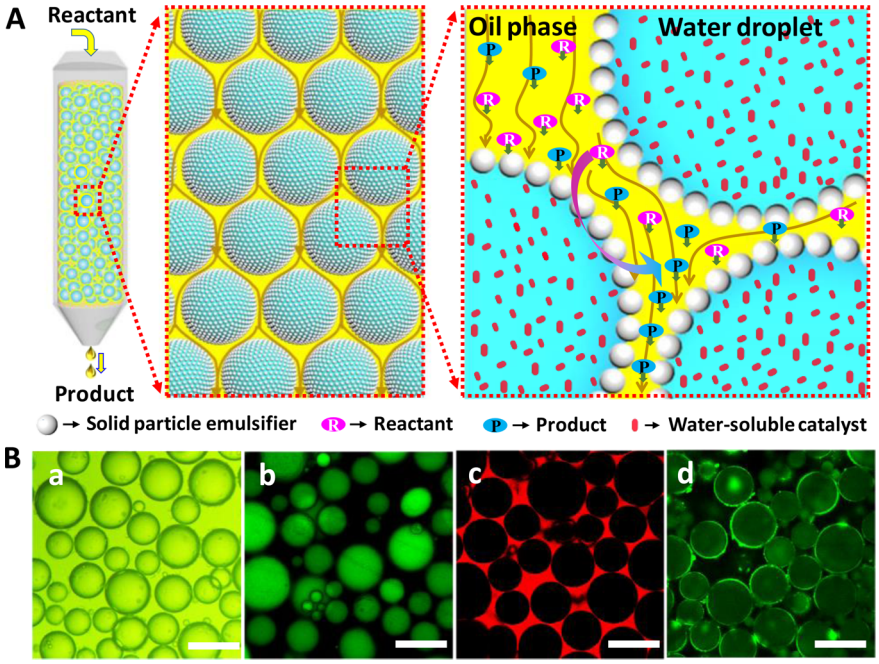

Figure 1. Schematic illustration of the Flow Pickering Emulsion strategy for organic–aqueous biphasic catalysis reactions (A) and characterization of the water-in-oil Pickering emulsion (B). (a) Optical microscopy image, (b) fluorescence confocal microscopy image with the water phase dyed by water-soluble FITC-dextran, (c) fluorescence confocal microscopy image with the oil phase dyed by oil-soluble Nile red, (d) fluorescence confocal microscopy image with the emulsifier dyed by fluorescein isothiocyanate isomer. Scale bar = 100 μm.

e.g., water droplets, can confine reagents of interest within them.[31−34] We envision that such compartmentalization of bulk water as water droplets and the network thus obtained may be helpful to process continuous flow biphasic catalysis in a rather simple manner if the droplets are effectively packed in a column reactor. This has not been explored up to now, although Pickering emulsion-based biphasic catalysis in batch reactions has been under extensive investigation recently.[35−50]

Capitalizing on the unique compartmentalization effects within a Pickering emulsion, herein we develop a conceptually novel method to access continuous flow liquid–liquid interface catalysis after addressing the underlying fundamental issues. As shown in Figure 1A, a typical biphasic system comprising an organic phase (oil phase), water phase and water-soluble catalyst is converted to a water-in-oil Pickering emulsion by adding a small amount of solid emulsifier. The bulk water phase is compartmentalized into water droplets within which the catalyst is distributed. This Pickering emulsion is then filled into a column reactor, at the bottom of which is a filter with micron-sized pores. Like solid particles in a conventional packed or fixed bed, the compartmentalized water droplets are densely packed in the column and do not leak out from the column since their size is larger than the pore size of the filter. The catalysts are thereby "immobilized" in the column due to the droplet confinement. The oil films between the droplets are interconnected spatially, thereby allowing the oil phase together with oil-soluble reactants to percolate through the packed droplet network due to gravity or applied pressure. During passage through the column reactor the reactants contact with the catalyst at the water–oil interface where catalytic reactions occur. Just as in the scenario of a conventional packed bed reaction, this Flow Pickering Emulsion (FPE) reaction allows reactants to be continuously fed from the inlet and products to be continuously collected at the outlet. The unique network originating from micron-scaled compartmentalization is responsible for high reaction efficiency. Besides overcoming an array of shortcomings of batch reactions, such continuous FPE catalysis represents an innovative liquid–liquid interface catalysis approach with an enhanced reaction efficiency effect. To our knowledge, it is the first attempt to translate batch biphasic catalysis to continuous flow catalysis in such an effective way.

2. RESULTS AND DISCUSSION

2.1. Fundamental Issues. To fulfill the above goal, there are three fundamental points that need to be elucidated: oil phase flow behavior, stability of the compartmentalized water droplets under flow and water droplet confinement capability toward water-soluble catalysts.

2.1.1. Oil Phase Flow. We used partially hydrophobic silica nanospheres as emulsifier to stabilize water-in-oil Pickering emulsions. This emulsifier was easily prepared through modification of hydrophilic silica nanospheres (40–60 nm in diameter) with methyltrimethoxysilane [Transmission Electron Microscopy (TEM) images, N_2 sorption isotherms and X-ray energy-dispersive spectrum (EDX) are displayed in Figure S1; an X-ray photoelectron spectrum (XPS) is shown in Figure S2; contact angle of a water drop in air on a pellet composed of the modified silica particles is determined as 93° in Figure S3]. A Pickering emulsion was prepared by stirring a mixture of water, *n*-octane (or toluene) and emulsifier for ca. 5 min (typically the water:oil volume ratio is 2:1), in which bulk water was compartmentalized into numerous droplets of 50–100 μm in diameter as evident from the optical microscopy image shown in Figure 1B, a. The emulsion type was confirmed to be water-in-oil through the fluorescence dyeing of the water and oil phases (Figure 1B, b and c). The location of emulsifier at the interface was confirmed by the fluorescence dyeing of the silica particle emulsifier (Figure 1B, d). Filling this as-prepared Pickering emulsion into a column reactor yielded a FPE

DOI: 10.1021/jacs.6b04265
J. Am. Chem. Soc. 2016, 138, 10173−10183

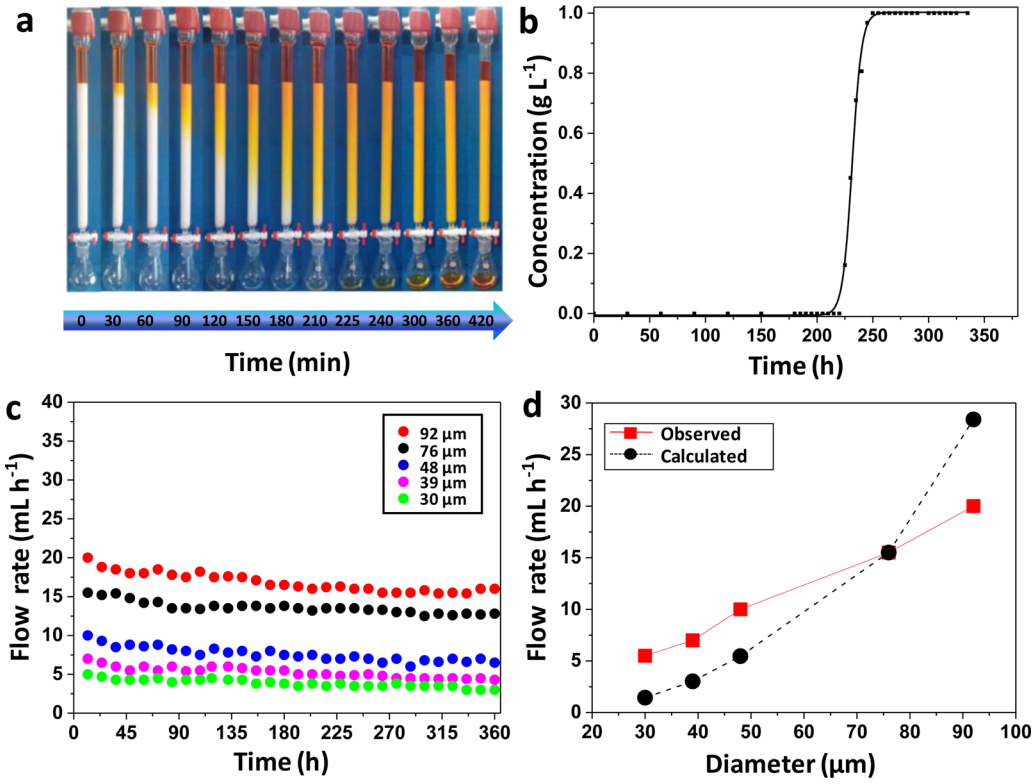

Figure 2. Flow behavior of the oil phase in the column. (a) Appearance of a flow Pickering emulsion column with oil phase stained by Sudan I (1 g L^{-1}) formulated with 18 mL of H_2O, 9 mL of *n*-octane and 0.36 g of particle emulsifier, 1.34 cm in the column diameter. (b) Concentration of Sudan I in the outflow at time *t*, 2 mL h^{-1}. (c) Variation of the oil phase flow rate with time for different average droplet sizes (filter pore diameter is 4−9 μm; the column diameter is 2 cm). The emulsions were formulated with 30 mL of H_2O, 15 mL of *n*-octane and particle emulsifier at 1, 2, 3, 4, or 5 wt % (with respect to water). (d) Theoretical (circles) and experimental (squares) points for the relationship between the oil phase flow rate and droplet size.

column whose height could be tuned by varying the total volume of the Pickering emulsion.

In order to visualize the flow of the oil phase in the column, we used a red dye (Sudan I) to stain *n*-octane since it is soluble in *n*-octane but not in water. The red-colored *n*-octane was continuously pumped into the column at a given velocity. As Figure 2a shows, immediately after the tap at the column bottom was opened (a few sec.), liquid was observed to flow out from the column. Meanwhile, the front of the red-colored *n*-octane layer began to enter the white Pickering emulsion layer leading to a yellow color which shifted downward with time. The yellow color was uniformly distributed in the column and its front was quite even. After 225 min, the colored front reached the column bottom and the red-colored *n*-octane eluted out from the column, and the concentration of Sudan I rapidly reached a maximum value before leveling off (Figure 2b). Notably, at any time, no clogs and faults were found at all. These results clearly indicate that it is very close to plug-flow behavior, which is further supported by the experiment of Sudan I residence time distribution (RTD) (Figure S4).[51,52] When the oil phase was changed to other organics such as benzene, toluene or *p*-xylene, the smooth flow behavior was also observed (Figure S5). In all these investigated cases, water was not found in the eluent. These experiments demonstrated that the oil phase together with molecules of interest could smoothly pass through the column, while the compartmentalized water droplets were fixed in the column reactor without any leakage as expected. In contrast, for surfactant-stabilized emulsions of the same droplet size, the compartmentalized water droplets were not fixed in the column but rather flowed out from the column with the oil phase (Figure S6), confirming the uniqueness of the compartmentalized effects of Pickering emulsions.

We speculate that the oil flow rate is related to the water droplet size. To validate this hypothesis, we packed a set of columns with droplets of different average size, achieved by adding different amounts of particle emulsifier. When the emulsifier amount was varied from 1 wt % to 5 wt %, the average droplet diameter decreased from 92 to 30 μm (Figure S7 and Table S1), consistent with previous findings.[53,54] The flow rates of oil in the FPE columns over a period of 360 h are plotted in Figure 2c. The oil flow rate is indeed dependent on the water droplet size. The initial flow rate declined from 20.1 mL h^{-1} to 5.2 mL h^{-1} as the droplet size decreased from 92 to 30 μm. This can be explained by the fact that at fixed volume fraction of water there is a larger number of water drops when they are small compared to when they are large, so oil has to flow around more drops when they are small slowing its flow rate.

To theoretically clarify the relationship between the oil flow rate and the droplet size, we develop an equation assuming that the compartmentalized droplets are solid microspheres. Based on the behavior in conventional packed beds,[55,56] eq 1 is derived for the volumetric flow rate driven by gravity (its derivation is provided in Figure S8):

$$V = \frac{\varepsilon^3}{180(1-\varepsilon)^2}\frac{S\rho g h_1}{\mu h_2}D^2 \quad (1)$$

DOI: 10.1021/jacs.6b04265
J. Am. Chem. Soc. 2016, 138, 10173−10183

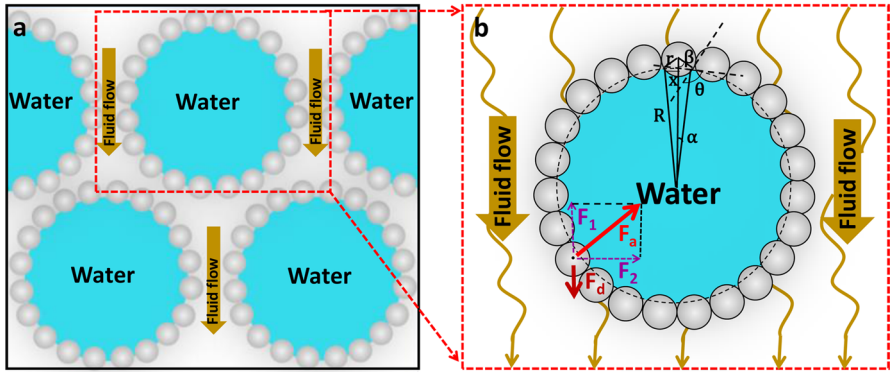

Figure 3. Force analysis for particles at the organic−aqueous interface. F_a represents the adsorption force, F_d represents the drag force, F_1 is the subsector of F_a in the vertical direction, F_2 is the subsector of F_a in the horizontal direction. x, r, R, α and β are the radius of the three-phase contact line, the particle radius, the emulsion droplet radius, a half center angle corresponding to arc of water droplet removed by the presence of the adsorbed solid particle and a half center angle corresponding to arc of solid particle immersed in water droplet, respectively.

in which ε is the voidage of the packed column, D is the droplet diameter, S is the cross sectional area of the column, ρ is the oil density, g is the acceleration due to gravity, μ is the oil viscosity, h_1 is the height of the oil phase (above the Pickering emulsion) and h_2 is the height of the Pickering emulsion. From eq 1, one can see that the flow rate is related to the droplet size as well as other parameters. This equation allows us to calculate a theoretical flow rate. It is interesting to find that the theoretical values of V are reasonably close to the experimentally determined ones (Figure 2d) and that they also increase as the droplet size increases. This is further support that the developed FPE column is indeed analogous to conventional solid particle-packed or fixed columns and the liquid flow rate of the FPE column can be explicitly tuned by changing the compartmentalized droplet size.

2.1.2. Stability of the Compartmentalized Water Droplets. Although it is well recognized that Pickering emulsions can be highly stable under quiescent conditions, their stability under oil flow conditions is less known. In fact, the experiments in Figure 2c and Figure S5 also demonstrate the high stability of FPE columns since the flow rate for each column was more or less constant over a period as long as 360 h. Moreover, after flowing for such a long time, the appearance of the Pickering emulsion and the droplet morphology were maintained as shown in Figure S9. No detectable water was found in the collected eluents even for a flow rate as high as 20.1 mL h^{-1}. These observations strongly suggest that the compartmentalized droplets of Pickering emulsions have sufficiently high stability against coalescence and macroscopic phase separation under oil flow conditions.

The high stability is also supported theoretically. As shown in Figure 3, particles at the interface are subjected to two kinds of force. One is the adsorption force holding particles at the water−oil interface (F_a, pointing to the droplet center) and the other is the drag force caused by the flow of the continuous phase liquid (F_d, pointing along the oil flow). The gravity and buoyancy forces are so small that they can be ignored as they are $<3 \times 10^{-18}$ N for a 60 nm-sized silica nanosphere.

The adsorption force F_a can be derived from the adsorption energy (ΔE, being the energy required to remove a particle from the interface).[25,57]

$$\Delta E = 2\pi\gamma_{ow}[r^2(1 + \cos\beta)\cos(\pi - \theta_{ow}) - R^2(1 - \cos\alpha)] \quad (2)$$

In eq 2, r is the particle radius, R is the emulsion droplet radius, γ_{ow} is the oil−water interfacial tension, θ_{ow} is the contact angle the particle makes with the oil−water interface and α and β (their definition is included in the footnote of Figure 3) can be calculated using the following equations.

$$\alpha = \arcsin\left(\frac{x}{R}\right);\ \beta = \arcsin\left(\frac{x}{r}\right);$$

$$x = \frac{rR\sin(\pi - \theta_{ow})}{\sqrt{r^2 + R^2 + 2rR\cos(\pi - \theta_{ow})}}$$

where x is the distance marked in Figure 3.

The immersion depth of the particle into water can be written as[58]

$$P_d = r(1 - \cos\beta) \quad (3)$$

Accordingly, F_a can be estimated as[58]

$$F_a = \frac{\Delta E}{P_d} \quad (4)$$

According to the parameters of the above Pickering emulsion, $R = 4.6 \times 10^{-5}$ m, $r = 3 \times 10^{-8}$ m, $\gamma_{ow} = 0.036$ N m^{-1}, and assuming θ_{ow} to be 120°, F_a is calculated as 5.2×10^{-9} N.

The drag force F_d can be calculated as outlined below. The constricted tube model was adopted to calculate the average diameter (d_c) of the spacing between droplets, the effective pore diameter ($d_{effective}$) and the maximum pore diameter (d_{max}):$d_c = \frac{2R}{2.5658}$; $d_{effective} = \frac{d_c}{0.470}$; $d_{max} = d_c 2.141$.[59]

The pore diameter change along the pore length (d_z) has been described by a parabolically shaped constricted tube:

$$d_z = d_c + 4(d_{max} - d_c)\left(0.5 - \frac{z}{h}\right)^2 \quad \left(0 < \frac{z}{h} < 1\right) \quad (5)$$

where z, h are the length along pore and pore length, respectively.

The number of pores in a cross-section of the bed is

$$N_{pore} = \frac{S_{column}\varepsilon}{(\pi/4)d_{effective}^2} \quad (6)$$

where ε is the voidage.

The concomitant shear experienced by a particle is

DOI: 10.1021/jacs.6b04265
J. Am. Chem. Soc. 2016, 138, 10173−10183

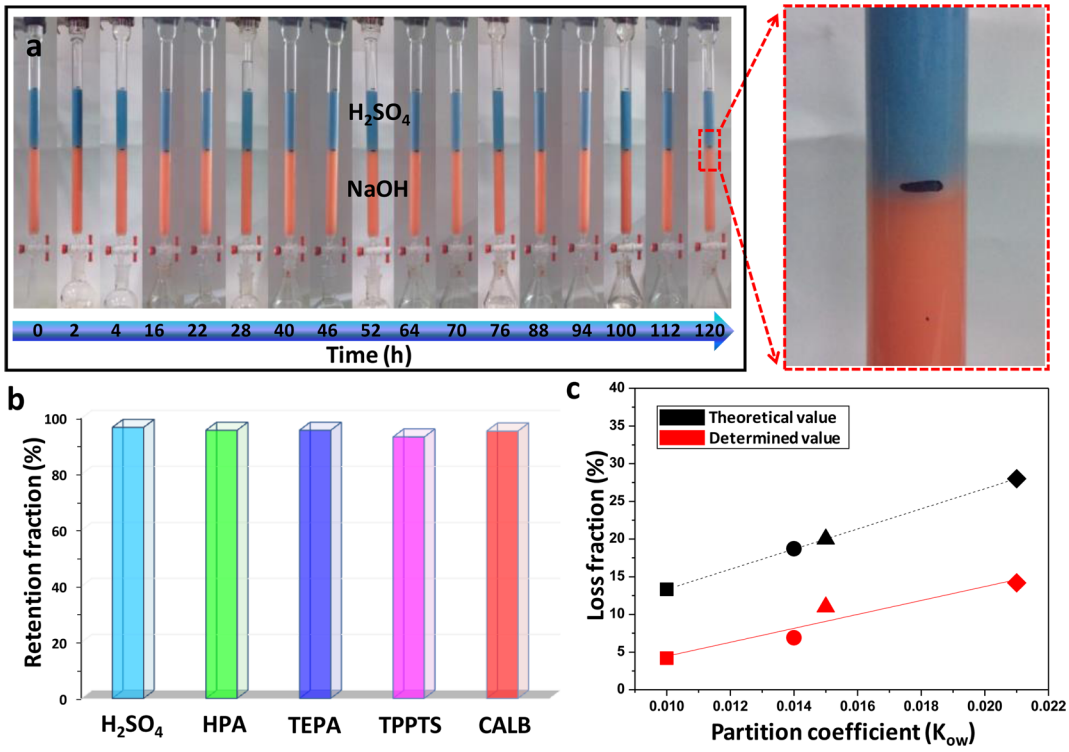

Figure 4. Droplet confinement ability toward water-soluble reagents. (a) Appearance of the Congo Red-stained FPE columns (1.34 cm in diameter) with 0.001 M H_2SO_4 confined in the upper layer and 0.001 M NaOH confined in the lower layer. The H_2SO_4-containing or NaOH-containing emulsions are formulated with 9 mL aqueous solution, 4.5 mL toluene and 0.18 g solid emulsifier. (b) Retention fraction of water-soluble reagents in the FPE column after 120 h flow (the detailed conditions are included in Supporting Information). (c) Theoretical (black) and experimental (red) correlation between the loss fraction after 120 h and the partition coefficient of water-soluble reagents. Square, circle, triangle and diamond represent TEPA, diethylenetriamine, ethylenediamine and ethanolamine, respectively.

$$\frac{\partial v}{\partial r} = \frac{V/N_{pore}}{(\pi/4)d_z^2}\frac{4(d_z/2 - r)}{(d_z/2)^2} \quad (7)$$

F_d can be estimated from

$$F_d = 10.205\pi\mu\left(\frac{\partial v}{\partial r}\right)r^2 \quad (8)$$

In this FPE column, the column diameter is 2 cm, the fluid flow rate in the packed column V = 20.1 mL h^{-1}, the oil dynamic viscosity $\mu = 0.52 \times 10^{-3}$ Pa s and the voidage of the packed column ε = 0.36 (for a packed bed by random packing of microspheres).[60] According to eq 7, the value of the hydrodynamic shear $\frac{\partial v}{\partial r}$ can be estimated to be 5.1−49.8 s^{-1} depending on the maximum and minimum values of d_z. Therefore, F_d is estimated to be in the range 7.47×10^{-16} -7.64×10^{-17} N.

Comparing the adsorption force F_a and the drag force F_d, we find that F_a is more than six orders of magnitude higher than F_d so that the subsector of F_a in the vertical direction is also much larger than F_d. The significant excess in the force balance guarantees the entrenched location of particles at the interface and permanent compartmentalization of water droplets, thereby avoiding droplet coalescence. In contrast, for the surfactant-stabilized emulsion, the surfactant molecule at the interface lacks such a strong adsorption force and dynamically exchanges with free surfactant molecules in the continuous phase.[61] The ineffective compartmentalization cannot prevent droplet coalescence and leakage from the column with the flowing oil phase. These theoretical results also support the fact that the compartmentalized droplets of Pickering emulsions have sufficiently high stability under flow conditions.

2.1.3. Confinement Ability of Water Droplets for Water-Soluble Reagents. In order to directly observe whether the water droplets themselves move significantly in the column reactor and whether the water-soluble reagents confined in the water droplets leach with the oil phase, we packed a column with two kinds of water-in-oil Pickering emulsion in the lower and upper layers, respectively. The aqueous phase in the lower layer contained NaOH and Congo Red (used as indicator that is soluble only in water, being azure at pH < 3.0 and red at pH > 5.0) and that in the upper layer contained H_2SO_4 and Congo Red. As seen in Figure 4a, the H_2SO_4-containing layer is azure and the NaOH-containing layer is red. In such an experiment, if the upper water droplets move downward with the oil phase, the color of the Pickering emulsion in the lower layer would change. At the beginning, there is a clear boundary between these two layers. After the oil phase flowed for 40 h (2 mL h^{-1}), this boundary was still distinct and had not moved in position. This is also the case even after 120 h (inset).

To quantitatively assess this confinement ability, we determined the residual H_2SO_4 concentration after a H_2SO_4-containing FPE flowed for 120 h (2 mL h^{-1}). It showed that 96.8% of the initial H_2SO_4 was retained in the column. When H_2SO_4 was replaced by the other highly water-soluble reagents (typical catalysts or catalyst ligands) such as heteropolyacid ($H_3PW_{12}O_{40}$, HPA) tetraethylenepentamine (TEPA), trisodium salt of tri-(*m*-sulfonphenyl)phosphine (TPPTS) and *Candida antarctica* enzyme (CALB, lipase), their retention fraction (ratio of the residual amount to the initial amount) was

DOI: 10.1021/jacs.6b04265
J. Am. Chem. Soc. 2016, 138, 10173−10183

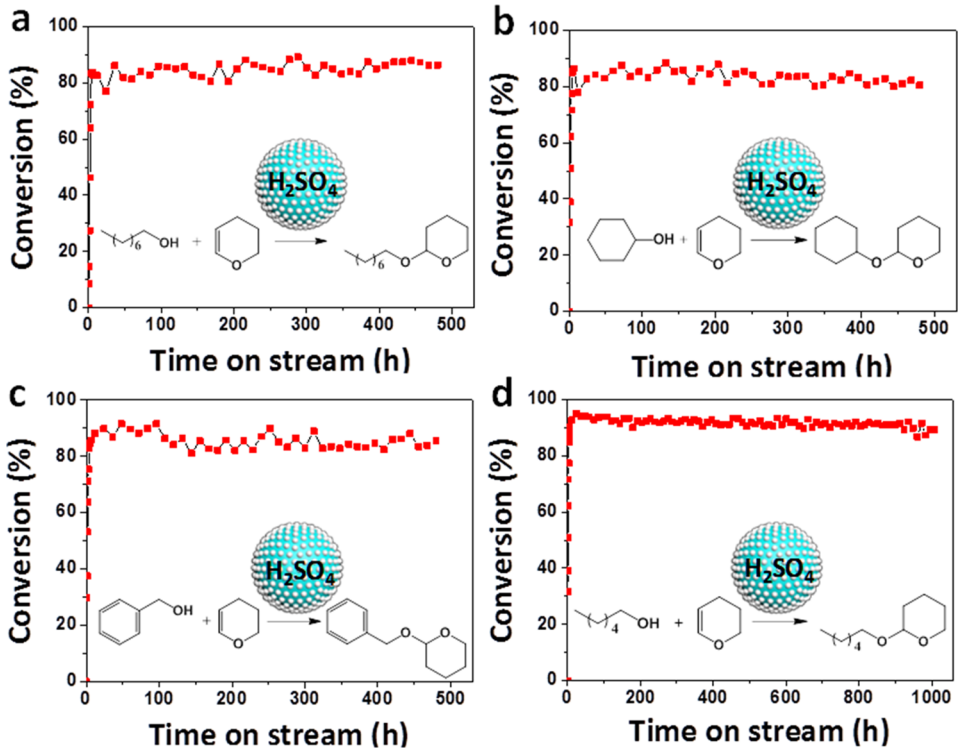

Figure 5. Plots of conversion against time in H_2SO_4-catalyzed addition reactions for the synthesis of tetrahydropyranyl ethers using the FPE method (the column is 1.34 cm in diameter). Reaction conditions: the Pickering emulsion is prepared with 1.8 mL of toluene, 3.6 mL of aqueous H_2SO_4 of a given concentration and 0.072 g of emulsifier; flow phase is a toluene solution of 0.25 M alcohol and 0.25 M 3,4-dihydro-2*H*-pyran, 50 °C, initial flow rate = 2 mL h^{-1}. (a) *n*-octanol, 0.5 M H_2SO_4, (b) cyclohexanol, 0.1 M H_2SO_4, (c) benzyl alcohol, 0.1 M H_2SO_4, (d) *n*-hexanol, 0.1 M H_2SO_4.

determined as 95.8%, 95.8%, 93.4% and 95.5% after continuous flow for 120 h, respectively (Figure 4b). These results confirm that the compartmentalized water droplets do not move with the flowing oil phase, which is due to their close packing in the column. It also confirms that the compartmentalized water droplets have excellent ability to confine water-soluble reagents against loss even under flow conditions.

To further unravel the factors governing the confinement effects, we deliberately examined a set of organic bases with different partition coefficients (K_{ow}) between toluene and water including TEPA, diethylenetriamine, ethylenediamine and ethanolamine, for which the partition coefficient between toluene and water ($[base]_{toluene}/[base]_{water}$) gradually increased (Figure S10).[62] It was found that the loss fraction (ratio of the amount of lost base to the amount of initial base) depends on the partition coefficient. The larger the partition coefficient is, the larger the loss fraction is. This is understandable because a higher partition coefficient implies that the base is more easily extracted to the oil phase. Interestingly, it was found that for all the investigated organic bases the determined loss fraction is much less than the theoretical loss fraction (Figure 4c), calculated using the partition coefficient. The considerable difference between the experimental loss fraction and the theoretical one was also confirmed by another set of experiments, in which the distance moved by the interface front in the column was measured (Figure S10). These data strongly indicate that in the FPE system the water-soluble reagents confined in the droplets are far away from partition equilibrium under the operating conditions, owing to the compartmentalized network.

2.2. Catalysis Applications. Since the above investigations demonstrate the high feasibility of our FPE strategy, we next apply it to biphasic catalysis reactions.

2.2.1. H_2SO_4-Catalyzed Addition Reaction. First, we chose sulfuric acid to examine the FPE strategy because it is extensively used in aqueous biphasic catalysis. A Pickering emulsion was prepared using the above silica particle emulsifier, toluene as continuous phase and H_2SO_4 (0.1 or 0.5 M) as dispersed phase. The H_2SO_4-catalyzed addition reaction of an alcohol with 3,4-dihydro-2*H*-pyran to form tetrahydropyranyl ethers is a frequently employed method for protecting alcohol groups.[63] The reactants and products are both oil-soluble. A solution of alcohol and 3,4-dihydro-2*H*-pyran in toluene was continuously pumped into the column reactor. The product-containing stream was collected from the bottom of the column and analyzed with GC at different times. The conversions were plotted as a function of time in Figure 5.

For *n*-octanol (Figure 5a) the conversion rapidly increased within the first few minutes and then leveled off between 80% and 87% (control experiment revealed that this reaction hardly occurs in the absence of H_2SO_4). In the 500 h monitored, the conversion was always maintained above 80% although the flow rate needed to be tuned from the initial 2 mL h^{-1} to the final 0.6 mL h^{-1} to obtain high conversion. It is found that the more uniform and smaller droplets lead to the higher reaction efficiency under the same conditions (Figure S11). This can be explained by the fact that the mondispersed, smaller droplet sizes have larger reaction interface area. For cyclohexanol and benzyl alcohol (Figure 5b and c), the FPE reactions also proceeded smoothly and their conversions were maintained above 78% and 81% over 500 h, respectively. More remarkably, even after the running time was extended to 1000 h for hexanol

DOI: 10.1021/jacs.6b04265
J. Am. Chem. Soc. 2016, 138, 10173−10183

(Figure 5d), a conversion of more than 90% was still achieved with the flow rate of the product stream varying between 2 mL h^{-1} and 0.6 mL h^{-1}. After such a long period, the emulsion droplet morphology and droplet sizes showed no significant change (Figure S12(a)). Moreover, it was found that 78% of the initial H_2SO_4 was retained. The high conversion over such a long time span and the good catalyst retention confirm the high feasibility of our FPE strategy to process continuous flow biphasic catalysis.

To get some insight into the catalysis occurring at compartmentalized interfaces, we carried out a set of FPE reactions in emulsions of different droplet sizes. The fine-tuning of droplet size was achieved by varying the amount of emulsifier, as described above. As the amount of emulsifier was increased from 0.5 wt % to 5 wt % (with respect to water), the average droplet diameter first decreased from 148 μm and then leveled off at ca. 42 μm (Figure S13).[53] On the basis of the conversion with time (Figure S14), the catalysis efficiency (CE, defined in footnote of Figure 6) was calculated as shown in Figure 6a. The CE first increased and then decreased as the amount of emulsifier increased. The FPE reaction using 3 wt % emulsifier exhibited the maximum CE value (0.292 mol mol^{-1} h^{-1}). This CE as a function of the amount of the solid emulsifier can be rationalized by inspecting Figure 6b. The increase in the emulsifier amount caused a decrease in the average droplet size, which results in an increase in the total oil–water interfacial area (S). In parallel, increasing the emulsifier amount is also accompanied by an increase in the coverage of emulsifier particles at droplet interfaces C (calculation is provided in Supporting Information),[64] also shown in Figure 6b. Higher coverage means that more silica particles are located at the compartmentalized droplet interface, forming two or even more particle layers. The high coverage compromised the possibility of the reactants (in oil) contacting with the catalyst (in water) and thereby led to a reduction in the CE. Hence, the trade-off between the droplet interfacial area and coverage by particles gives rise to a maximum catalysis efficiency that is obtained in the cross over region of the two plots, as shown in Figure 6b. Such a compromise provides a clue to tune catalysis efficiency through changing the liquid–liquid interface properties.

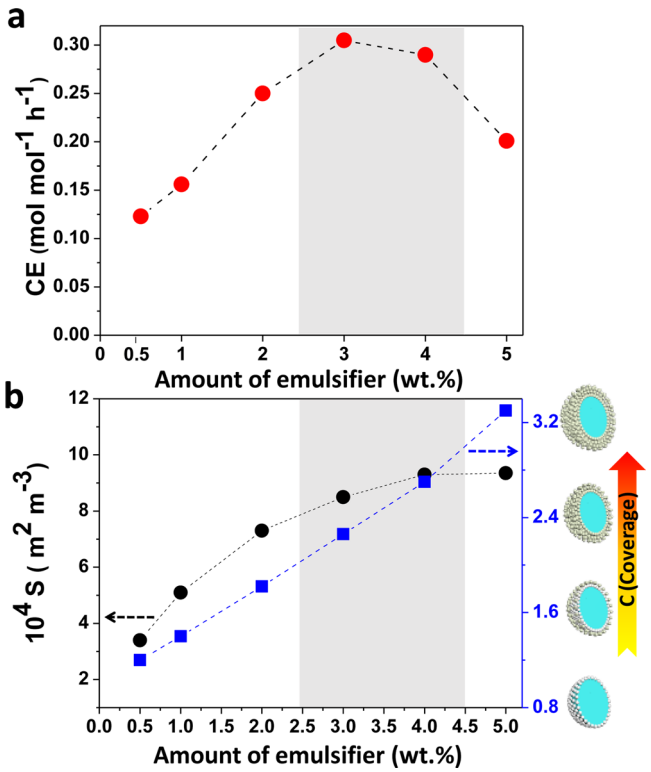

Figure 6. Relationship between the FPE catalysis efficiency of the addition of *n*-octanol with 3,4-dihydro-2*H*-pyran and interface properties. The flow rate was maintained at 2.5 mL h^{-1}. Other reaction conditions are the same as in Figure 5a. (a) Catalysis efficiency (CE) vs emulsifier amount. CE is defined as the moles of converted reactants per mole of catalyst per h (mol mol^{-1} h^{-1}), calculated after the conversion leveled off (above 5 h). (b) Oil–water interfacial area S and coverage of interface by particles C vs emulsifier amount.

2.2.2. HPA-Catalyzed Ring Opening Reactions. We chose another widely used water-soluble catalyst heteropolyacid (HPA, $H_3PW_{12}O_{40}$) to further examine the FPE reaction. The ring opening of an epoxide with an aromatic amine to form a β-amino alcohol was investigated because amino alcohols are organic compounds of considerable use in medicinal chemistry.[65] An HPA-containing FPE column was obtained using an aqueous HPA solution as dispersed phase, toluene as continuous phase and silica particles as emulsifier. The toluene solution of epoxide and aromatic amine was pumped into the column at a given rate and the product β-amino alcohol in toluene was collected from the column outlet. For all the investigated substrates such as 4-methylaniline, 4-isopropylaniline and 4-methoxyaniline, the FPE reactions proceeded efficiently. As high as 87–99% conversions were obtained after a short period of time and were maintained over 500 h (Figure 7a, b and c), albeit at the expense of the flow rate (decreasing from 1.5 mL h^{-1} to 0.9 mL h^{-1}). Even during 1000 h of examination (Figure 7d), a conversion of aniline remained at >86% with the flow rate in the range of 3.0–1.0 mL h^{-1}.

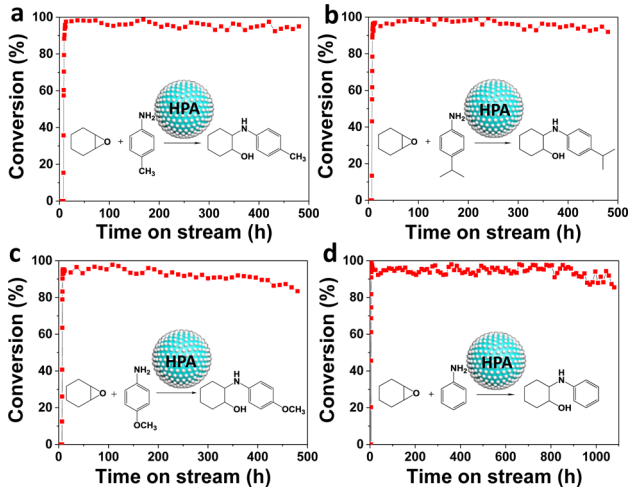

Figure 7. HPA-catalyzed ring opening reactions of epoxides with anilines using the FPE method (the column is 3.6 cm in diameter). The Pickering emulsions consist of 30 mL HPA aqueous solution (0.01 M), 15 mL of toluene and 0.9 g of emulsifier. Reaction conditions: 0.5 M amines and 0.5 M cyclohexene oxide in toluene, 50 °C. (a) 4-methylaniline with initial flow rate of 1.5 mL h^{-1}, (b) 4-isopropylaniline with initial flow rate of 1.5 mL h^{-1}, (c) 4-methoxyaniline with initial flow rate of 1.5 mL h^{-1}, (d) aniline with initial flow rate of 3 mL h^{-1}.

DOI: 10.1021/jacs.6b04265
J. Am. Chem. Soc. 2016, 138, 10173–10183

After such a long reaction time, the droplet morphology and sizes remained unchanged (Figure S12(b)) and 73% of HPA was retained in the column. The HPA case study further confirmed the generality and versatility of our FPE reactions.

2.2.3. Enzyme-Catalyzed Reaction. We further test the applicability of the FPE strategy with an enzyme that is highly water-soluble. *Candida antarctica* lipase B (CALB) promoting the kinetic resolution of racemic esters to chiral alcohol was used as a model reaction.[66−68] Similar to the above procedure, a packed column with CALB confined in water droplets dispersed in oil was achieved. Soon after racemic 4-methyl-2-pentanol acetates dissolved in *n*-octane were introduced into the column, the products including chiral alcohol and chiral ester in the eluent were detected. The enantiomeric excess (ee) of 4-methyl-2-pentanol was above 99% and the ee value of acetate was more than 95%. After continuous running for as long as 720 h (Figure 8a), their ee values showed no apparent

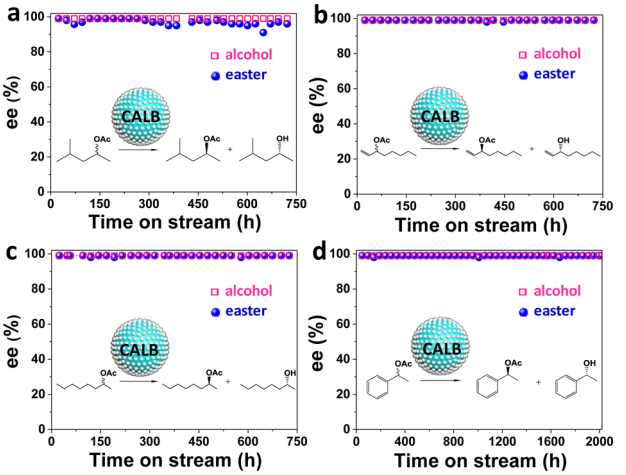

Figure 8. CALB enzyme-catalyzed hydrolysis kinetic resolution of racemic acetates using the FPE method (the column is 3.6 cm in diameter). The Pickering emulsions were formulated with 40 mL aqueous enzyme (0.1 mg mL^{-1}, 0.5 M Na_2HPO_4), 20 mL *n*-octane and 1.2 g emulsifier. Reaction conditions: 0.25 M racemic acetates in *n*-octane as flow phase, 35 °C. (a) 4-Methyl-2-pentanol acetate, initial flow rate 1.0 mL h^{-1}, (b) 1-octen-3-ol acetate, initial flow rate 1.5 mL h^{-1}, (c) 2-octanol acetate, initial flow rate 2.0 mL h^{-1}, (d) 1-phenylethyl acetate, initial flow rate 4 mL h^{-1}.

decrease and the streamflow rate was maintained in the range of 1.0−0.7 mL h^{-1}. For the other substrates such as racemic 1-octen-3-ol acetate and 2-octanol acetate, the ee values of the corresponding chiral alcohol and chiral ester exceeded 98% (Figure 8b and c), while a relatively steady flow rate was also achieved. To further check the potential of the FPE strategy, we extended the time scale to 2000 h. Strikingly, ee values as high as 98% for alcohol and ester were still achieved in the case of 1-phenylethyl acetate (Figure 8d) although the flow rate of the stream needed to be tuned from the initial 4 mL h^{-1} to the final 1 mL h^{-1} (every time the collected eluent reached 400 mL, the Pickering emulsion was subjected to demulsification for supplying water and tuning pH because water as a reactant in this reaction was consumed and acetic acid was released from the reaction to lower the pH). 136 g of racemic 1-phenylethyl acetate was successfully resolved to 48 g of enantiopure alcohol and 65 g of enantiopure 1-phenylethyl acetate. It can be estimated that each mg of protein of CALB can resolve 34 g of ester, highlighting high productivity of the enzymatic FPE reactions. This case study further consolidates the generality, versatility and excellent durability of our FPE reactions.

3. FURTHER DISCUSSION

We further identified the FPE reaction superiority in terms of catalysis efficiency through benchmarking the existing batch biphasic systems including an agitation-free biphasic reaction, a stirred biphasic reaction, the recently developed agitation-free Pickering emulsion reaction[54] and a stirred Pickering emulsion reaction (Figure 9A). Based on the kinetic plot of each H_2SO_4-catalyzed addition reaction of *n*-octanol with 3,4-dihydro-2*H*-pyran (Figure 9B), the catalysis efficiency (CE) was calculated (Figure 9C). The agitation-free biphasic reaction gave a CE of 0.0013 mol mol^{-1} h^{-1}. This value is dramatically improved up to 0.0106 mol mol^{-1} h^{-1} when implementing agitation. When the biphasic system is transferred to an agitation-free Pickering emulsion system, CE was further improved up to 0.023 mol mol^{-1} h^{-1}. The improved reaction interface area results in higher catalysis efficiency.[21] For the Pickering emulsion reaction employing agitation (900 rpm), CE was 0.024 mol mol^{-1} h^{-1}. The sufficiently large reaction interface area makes agitation unnecessary for Pickering emulsion reactions, which is consistent with our prior findings.[54] Notably, the developed FPE reaction gave a CE of 0.235 mol mol^{-1} h^{-1}, about 20 times higher than those of the conventional batch stirred biphasic reaction (900 rpm), and 10 times higher than the batch Pickering emulsion reaction. Such striking comparisons highlight the exceptionally high catalysis efficiency of the FPE reactions.

The catalysis efficiency enhancement effects were also found in the HPA-catalyzed ring opening reactions and CALB-catalyzed kinetic resolution reaction. In the HPA-catalyzed ring opening reaction, the catalysis efficiency of the FPE systems is about twice that of the Pickering emulsions with or without agitation, and is much higher than that of the conventional biphasic systems with agitation (Figure S15). In the CALB-catalyzed kinetic resolution reaction, the FPE reaction also exhibited the highest specific activity among these five systems (Figure S16). These comparisons unanimously demonstrate a general trend that the FPE concept allows biphasic systems to access the highest catalysis efficiency.

Notably, for the H_2SO_4-catalyzed addition reaction in the FPE system, more than 1 order of magnitude catalysis efficiency enhancement should not be simply attributed to mass transport enhancement. To verify this, we further examined the batch H_2SO_4-catalyzed addition reactions under mass transport limitation-free conditions (mass transport limitation was eliminated by increasing the agitation speed). The kinetic profiles for batch Pickering emulsion systems and conventional biphasic reactions are provided in Figure 9D and E, respectively. For the batch Pickering emulsion reactions, the reaction rate had no apparent change when the agitation speed was increased progressively from 900 to 1800 rpm, indicating that batch Pickering emulsion reactions were not limited by mass transport. The catalysis efficiency has a maximum value (CE_{max}) just at the beginning of reaction, as given by the slope in Figure 9d. It is 0.041 mol mol^{-1} h^{-1}, which is only approximately 1/6 of the CE of the FPE reaction calculated at steady state. For the conventional batch reactions, the reaction rate increased with an increase in the agitation speed up to 1500 rpm. This indicates that the reaction is no longer limited by mass transport when the agitation speed exceeds this value. On this occasion, the catalysis efficiency reached a maximum

DOI: 10.1021/jacs.6b04265
J. Am. Chem. Soc. 2016, 138, 10173−10183

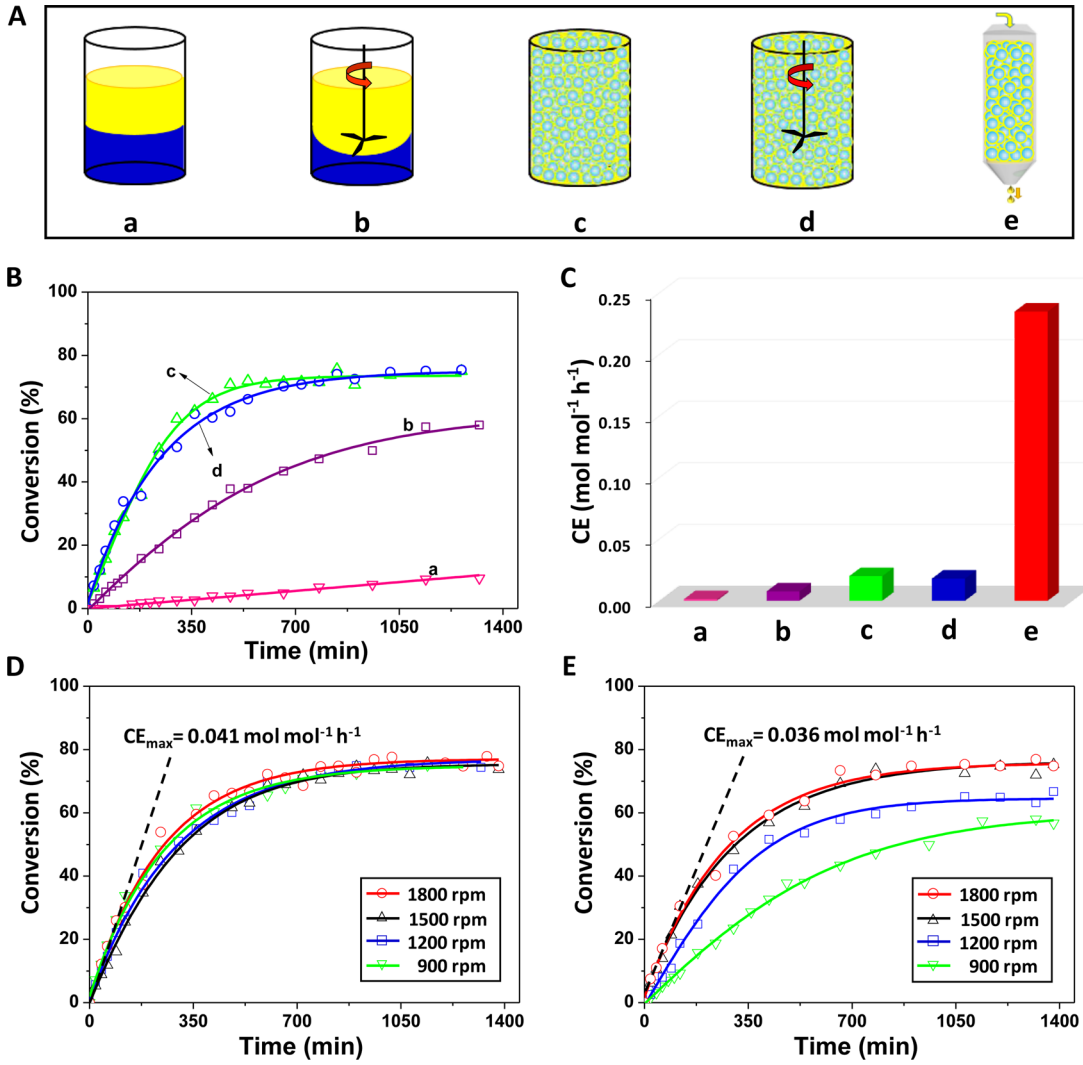

Figure 9. Comparison of the H_2SO_4-catalyzed addition of *n*-octanol with 3,4-dihydro-2*H*-pyran using the existing biphasic batch reactions and using the FPE reaction. (A) Cartoon representation of various reaction systems. (a) Agitation-free biphasic reaction, (b) biphasic reaction with agitation speed of 900 rpm, (c) agitation-free Pickering emulsion reaction, (d) Pickering emulsion reaction with agitation speed of 900 rpm, (e) FPE reaction. Batch reaction conditions: 8 mL aqueous H_2SO_4 (0.5 M), 4 mL reactant solution in toluene (0.25 M), 50 °C, 0.16 g emulsifier if needed. The reaction conditions of the FPE system are the same as in Figure 5a except the flow rate = 2.5 mL h^{-1}. (B) Kinetic reaction profile with time for the batch reactions. (C) Catalysis efficiency (CE) of the batch reactions over 550 min and the FPE reaction after the conversion leveled off. (D) Batch Pickering emulsion systems at different agitation speeds. The maximum catalysis efficiency (CE_{max}) is given under the mass transport limitation-free conditions calculated at the beginning of reaction. (E) Conventional batch biphasic systems at different agitation speeds.

value (CE_{max} = 0.036 mol mol^{-1} h^{-1}), close to that of the Pickering emulsion system and also about 1/6 of that for the FPE reaction. It is the same case with the HPA-catalyzed ring opening reactions, where the CE of the FPE reactions is also higher than the CE_{max} of the batch reaction (Figure S15D). These data support the hypothesis that the catalysis efficiency enhancement in the FPE system is not simply due to the fast mass transport, but rather suggests that there exists a flow catalysis effect. This effect may originate from the flowing oil that promotes the release of product molecules from the catalyst at the liquid−liquid interface and its speedy removal from the reaction system.[18,69] According to Le Chatelier's principle,[70] the immediate removal of the product from the catalytic sites and the reaction systems is beneficial to decrease any inhibitory effect of the product and shift the reaction equilibrium, thus "pushing" the reaction forward. This is supported by the results in which the conversion of *n*-octanol in the FPE system is higher than that in the batch reaction (>80% vs 76%).

4. CONCLUSIONS

We put forward a conceptually novel method for continuous flow liquid−liquid interface catalysis on the basis of compartmentalization effects of a Pickering emulsion (namely FPE), established the theoretical framework and then successfully applied the strategy in biphasic catalysis reactions. It has been experimentally and theoretically demonstrated that the FPE method allows the oil phase containing reactant molecules to continuously pass through the column in a manner of plug-type flow, still retaining the compartmentalized water droplet integrity and the water-soluble reagent in the column reactor. The flow rate is found to be highly dependent on the droplet size. For highly water-soluble reagents, the FPE system exhibits excellent confinement ability against loss. The success lies in the fact that the interfacial adsorption force

DOI: 10.1021/jacs.6b04265
J. Am. Chem. Soc. 2016, 138, 10173−10183

acting on the particles of solid emulsifier is significantly larger than the drag force caused by the oil flow. The FPE method is successfully applied in three different types of reactions including H_2SO_4-catalyzed addition reactions, HPA-catalyzed ring opening reactions and enzyme-catalyzed chiral reactions which demonstrate the generality and versatility of the FPE method. In comparison to conventional batch counterparts, the FPE reaction features a higher level of green footprint because it avoids continuous agitation and intermittent separation of product with catalyst. Impressively, the FPE reactions exhibit not only excellent durability even over a span as long as 2000 h, but also significantly enhanced catalysis efficiency in comparison to the existing aqueous biphasic systems, suggesting a novel flow liquid−liquid interface catalysis effect. Being operationally simple and efficient, our FPE method provides an unprecedented opportunity for practical applications of biphasic catalysis and the unique flow liquid−liquid interface for designing innovative catalysis systems. Moreover, the strategy regarding compartmentalization of a bulk liquid phase for continuous flow could be extended to other biphasic systems such as ionic liquid−oil and ionic liquid−water and other biphasic processes such as extraction and separation.

■ ASSOCIATED CONTENT

Supporting Information

The Supporting Information is available free of charge on the ACS Publications website at DOI: 10.1021/jacs.6b04265.

Experimental details; TEM images; Water contact angles; Appearance of Pickering emulsions; Droplet size distributions; Optical microscopy image; Theoretical model; Equation derivation process; Reaction kinetics monitoring and MS data for products. (PDF)

■ AUTHOR INFORMATION

Corresponding Author

*hqyang@sxu.edu.cn

Notes

The authors declare no competing financial interest.

■ ACKNOWLEDGMENTS

The authors thank Dr. R. Ettelaie, University of Leeds, for his help with the partial theoretical analysis. This work is supported by the Natural Science Foundation of China (21573136 and U1510105) and the Program for New Century Excellent Talents in University (NECT-12-1030).

■ REFERENCES

(1) Tundo, P.; Perosa, A. *Chem. Soc. Rev.* **2007**, *36*, 532.
(2) Li, C. J.; Chen, L. *Chem. Soc. Rev.* **2006**, *35*, 68.
(3) Minakata, S.; Komatsu, M. *Chem. Rev.* **2009**, *109*, 711.
(4) Joó, F. *Acc. Chem. Res.* **2002**, *35*, 738.
(5) Yang, H. Q.; Zhou, T.; Zhang, W. J. *Angew. Chem., Int. Ed.* **2013**, *52*, 7455.
(6) Cole-Hamilton, D. J. *Science* **2003**, *299*, 1702.
(7) Liu, S. F.; Xiao, J. L. *J. Mol. Catal. A: Chem.* **2007**, *270*, 1.
(8) Cents, A. H. G.; Brilman, D. W. F.; Versteeg, G. F. *Ind. Eng. Chem. Res.* **2004**, *43*, 7465.
(9) Tsubogo, T.; Oyamada, H.; Kobayashi, S. *Nature* **2015**, *520*, 329.
(10) Gutmann, B.; Cantillo, D.; Kappe, C. O. *Angew. Chem., Int. Ed.* **2015**, *54*, 6688.
(11) Booker-Milburn, K. *Nat. Chem.* **2012**, *4*, 433.
(12) Hartman, R. L.; McMullen, J. P.; Jensen, K. F. *Angew. Chem., Int. Ed.* **2011**, *50*, 7502.
(13) Wiles, C.; Watts, P. *Green Chem.* **2012**, *14*, 38.
(14) Hafez, A. M.; Taggi, A. E.; Dudding, T.; Lectka, T. *J. Am. Chem. Soc.* **2001**, *123*, 10853.
(15) Valera, F. E.; Quaranta, M.; Moran, A.; Blacker, J.; Armstrong, A.; Cabral, J. T.; Blackmond, D. G. *Angew. Chem., Int. Ed.* **2010**, *49*, 2478.
(16) Vaccaro, L.; Lanari, D.; Marrocchi, A.; Strappaveccia, G. *Green Chem.* **2014**, *16*, 3680.
(17) Kobayashi, J.; Mori, Y.; Okamoto, K.; Akiyama, R.; Ueno, M.; Kitamori, T.; Kobayashi, S. *Science* **2004**, *304*, 1305.
(18) Mason, B. P.; Price, K. E.; Steinbacher, J. L.; Bogdan, A. R.; McQuade, D. T. *Chem. Rev.* **2007**, *107*, 2300.
(19) Elvira, K. S.; Solvas, X. C. i.; Wootton, R. C. R.; deMello, A. J. *Nat. Chem.* **2013**, *5*, 905.
(20) Yoshida, J.; Kim, H.; Nagaki, A. *ChemSusChem* **2011**, *4*, 331.
(21) Nieves-Remacha, M. J.; Kulkarni, A. A.; Jensen, K. F. *Ind. Eng. Chem. Res.* **2012**, *51*, 16251.
(22) Arhancet, J. P.; Davis, M. E.; Merola, J. S.; Hanson, B. E. *Nature* **1989**, *339*, 454.
(23) Zoumpanioti, M.; Stamatis, H.; Xenakis, A. *Biotechnol. Adv.* **2010**, *28*, 395.
(24) Yan, N. X.; Gray, M. R.; Masliyash, J. H. *Colloids Surf., A* **2001**, *193*, 97.
(25) Aveyard, R.; Binks, B. P.; Clint, J. H. *Adv. Colloid Interface Sci.* **2003**, *100−102*, 503.
(26) Tsuji, S.; Kawaguchi, H. *Langmuir* **2008**, *24*, 3300.
(27) Read, E. S.; Fujii, S.; Amalvy, J. I.; Randall, D. P.; Armes, S. P. *Langmuir* **2004**, *20*, 7422.
(28) Tu, F.; Lee, D. *J. Am. Chem. Soc.* **2014**, *136*, 9999.
(29) Liang, F. X.; Shen, K.; Qu, X. Z.; Zhang, C. L.; Wang, Q.; Li, J. L.; Liu, J. G.; Yang, Z. Z. *Angew. Chem., Int. Ed.* **2011**, *50*, 2379.
(30) Du, K.; Glogowski, E.; Emrick, T.; Russell, T. P.; Dinsmore, A. D. *Langmuir* **2010**, *26*, 12518.
(31) Dewey, D. C.; Strulson, C. A.; Cacace, D. N.; Bevilacqua, P. C.; Keating, C. D. *Nat. Commun.* **2014**, *5*, 4670.
(32) Chandrawati, R.; van Koeverden, M. P.; Lomas, H.; Caruso, F. *J. Phys. Chem. Lett.* **2011**, *2*, 2639.
(33) Li, M.; Harbron, R. L.; Weaver, J. V. M; Binks, B. P.; Mann, S. *Nat. Chem.* **2013**, *5* (5), 529.
(34) Yang, H. Q.; Fu, L. M.; Wei, L. J.; Liang, J. F.; Binks, B. P. *J. Am. Chem. Soc.* **2015**, *137*, 1362.
(35) Crossley, S.; Faria, J.; Shen, M.; Resasco, D. E. *Science* **2010**, *327*, 68.
(36) Zapata, P. A.; Faria, J.; Ruiz, M. P.; Jentoft, R. E.; Resasco, D. E. *J. Am. Chem. Soc.* **2012**, *134*, 8570.
(37) Pera-Titus, M.; Leclercq, L.; Clacens, J. M.; De Campo, F.; Nardello-Rataj, V. *Angew. Chem., Int. Ed.* **2015**, *54*, 2006.
(38) Piradashvili, K.; Alexandrino, E. M.; Wurm, F. R.; Landfester, K. *Chem. Rev.* **2016**, *116*, 2141.
(39) Chen, Z. W.; Zhou, L.; Bing, W.; Zhang, Z. J.; Li, Z. H.; Ren, J. S.; Qu, X. G. *J. Am. Chem. Soc.* **2014**, *136*, 7498.
(40) Yang, Y. L.; Zhou, W. J.; Liebens, A.; Clacens, J. M.; Pera-Titus, M.; Wu, P. *J. Phys. Chem. C* **2015**, *119*, 25377.
(41) Zhou, W. J.; Fang, L.; Fan, Z. Y.; Albela, B.; Bonneviot, L.; De Campo, F.; Pera-Titus, M.; Clacens, J. M. *J. Am. Chem. Soc.* **2014**, *136*, 4869.
(42) Wu, C. Z.; Bai, S.; Ansorge-Schumacher, M. B.; Wang, D. Y. *Adv. Mater.* **2011**, *23*, 5694.
(43) Zhao, Y. P.; Zhang, X. M.; Sanjeevi, J.; Yang, Q. H. *J. Catal.* **2016**, *334*, 52.
(44) Potier, J.; Menuel, S.; Chambrier, M. H.; Burylo, L.; Blach, J. F.; Woisel, P.; Monflier, E.; Hapiot, F. *ACS Catal.* **2013**, *3*, 1618.
(45) Wang, Z. P.; van Oers, M. C. M.; Rutjes, F. P. J. T.; van Hest, J. C. M. *Angew. Chem., Int. Ed.* **2012**, *51*, 10746.
(46) Shan, Y. Y.; Yu, C.; Yang, J.; Dong, Q.; Fan, X. M.; Qiu, J. S. *ACS Appl. Mater. Interfaces* **2015**, *7*, 12203.
(47) Jing, R.; Tang, J.; Zhang, Q.; Chen, L.; Ji, D. X.; Yu, F. W.; Lu, M. Z.; Ji, J. B.; Wang, J. L. *Chem. Eng. J.* **2015**, *280*, 265.

DOI: 10.1021/jacs.6b04265
J. Am. Chem. Soc. 2016, 138, 10173−10183

(48) Zhang, C.; Hu, C. Y.; Zhao, Y. L.; Möeller, M.; Yan, K.; Zhu, X. M. *Langmuir* **2013**, *29*, 15457.
(49) Tan, H. Y.; Zhang, P.; Wang, L.; Yang, D.; Zhou, K. B. *Chem. Commun.* **2011**, *47*, 11903.
(50) Huang, J. P.; Cheng, F. Q.; Binks, B. P.; Yang, H. Q. *J. Am. Chem. Soc.* **2015**, *137*, 15015.
(51) Carneiro, O. S.; Covas, J. A.; Ferreira, J. A.; Cerqueira, M. F. *Polym. Test.* **2004**, *23*, 925.
(52) Puaux, J. P.; Bozga, G.; Ainser, A. *Chem. Eng. Sci.* **2000**, *55*, 1641.
(53) Frelichowska, J.; Bolzinger, M. A.; Chevalier, Y. *J. Colloid Interface Sci.* **2010**, *351*, 348.
(54) Zhang, W. J.; Fu, L. M.; Yang, H. Q. *ChemSusChem* **2014**, *7*, 391.
(55) Slattery, J. C. *AIChE J.* **1967**, *13*, 1066.
(56) Nakayama, A.; Kuwahara, F.; Sano, Y. *AIChE J.* **2007**, *53*, 732.
(57) Aveyard, R.; Clint, J. H.; Horozov, T. S. *Phys. Chem. Chem. Phys.* **2003**, *5*, 2398.
(58) Dudchenko, A. V.; Rolf, J.; Shi, L.; Olivas, L.; Duan, W. Y.; Jassby, D. *ACS Nano* **2015**, *9*, 9930.
(59) Bergendahl, J.; Grasso, D. *Chem. Eng. Sci.* **2000**, *55*, 1523.
(60) Dodds, J. A. *J. Colloid Interface Sci.* **1980**, *77*, 317.
(61) Skartlien, R.; Sollum, E.; Schumann, H. *J. Chem. Phys.* **2013**, *139*, 174901.
(62) Dunstan, T. S.; Fletcher, P. D. I. *Langmuir* **2011**, *27*, 3409.
(63) Wiles, C.; Watts, P. *Chem. Commun.* **2007**, 4928.
(64) Gautier, F.; Destribats, M.; Perrier-Cornet, R.; Dechézelles, J. F.; Giermanska, J.; Héroguez, V.; Ravaine, S.; Leal-Calderon, F.; Schmitt, V. *Phys. Chem. Chem. Phys.* **2007**, *9*, 6455.
(65) Saikia, L.; Satyarthi, J. K.; Srinivas, D.; Ratnasamy, P. *J. Catal.* **2007**, *252*, 148.
(66) Steudle, A. K.; Subinya, M.; Nestl, B. M.; Stubenrauch, C. *Chem. - Eur. J.* **2015**, *21*, 2691.
(67) Verho, O.; Bäckvall, J. E. *J. Am. Chem. Soc.* **2015**, *137*, 3996.
(68) Wu, Q.; Soni, P.; Reetz, M. T. *J. Am. Chem. Soc.* **2013**, *135*, 1872.
(69) El Kadib, A.; Chimenton, R.; Sachse, A.; Fajula, F.; Galarneau, A.; Coq, B. *Angew. Chem., Int. Ed.* **2009**, *48*, 4969.
(70) Armor, J. N. *Appl. Catal., A* **2001**, *222*, 91.

DOI: 10.1021/jacs.6b04265
J. Am. Chem. Soc. 2016, 138, 10173−10183